# INVESTIGATION INTO THE USE OF PULSED FOCUSED ULTRASOUND AS A METHOD OF FACILITATING HOMING OF UMBILICAL CORD BLOOD STEM CELLS AFTER SYSTEMIC ADMINISTRATION IN ISCHEMIC STROKE RAT MODELS

A THESIS

SUBMITTED TO THE FACULTY OF THE

UNIVERSITY OF MINNESOTA

BY

JOSHUA DANIEL HAMBORG

IN PARTIAL FULFILLMENT OF THE REQUIREMENTS

FOR THE DEGREE OF

MASTER OF SCIENCE IN STEM CELL BIOLOGY

WALTER C. LOW, PHD, ADVISOR

APRIL 2016

# Acknowledgements


- All experiments made possible through Dr. Walter Low and Dr. Emad Ebbini of the University of Minnesota
- Experiments with pFUS performed by Dr. Emad Ebbini and Dr. DaLong Lui of the University of Minnesota's Electrical and Computer Engineering Department with the assistance of Neelu Choudhary and Juan Du
- Tissue processing assistance provided by Colleen Forster of the University of Minnesota's Histology and IHC Laboratory
- Animal experiment onsite supervision conducted by Meri DuRand and Nicholas Burrows of the Research Animal Resources Department of the University of Minnesota
- Additional assistance with experimental design and execution provided by Holly Hewitt, MS, Andrew Crane, PhD, Vibha Savanur, MS, and Kyle Schaible, of the University of Minnesota Walter Low and Andrew Grande Laboratories

# Abstract

Stroke is a leading cause of mortality with no current therapies for chronic stroke victims. Our work investigates how to help chronic stroke patients regain function lost due to their stroke. This was accomplished by exploring how the use umbilical cord blood stem cells (UCBSCs), used in conjunction with pulsed focused ultrasound (pFUS), could provide a safe, efficient, and relatively non-invasive method for providing neuroregenerative therapy. Using rat stroke models that have undergone unilateral MCA occlusion, we propose that tail vein injections of UCBSCs, followed immediately afterwards by pFUS targeted to regions of ischemic damage, will result in functional improvements due to engraftment and neural differentiation of the stem cells. Initial immunohistochemical analysis of control rat brain tissue investigated how the local neuro-environment may become therapeutically favorable after transcranial pFUS treatments. Results obtained so far are preliminary.

# Table of Contents

# List of Figures

# Introduction

Stroke, a neurological event caused by disrupted cerebral circulation, is a leading cause of mortality and morbidity throughout the world. In the United States, a stroke occurs every 40 seconds, and there is a stroke related death every 4 minutes (Moskowitz et al., 2010). Of those who survive a stroke, 70% become compromised in their capacity to work, and 30% need assistance with self-care (Moskowitz et al., 2010). Unfortunately, there are no therapies that have been shown to significantly improve the functional status of stroke patients (Teasell et al., 2009). The only approved therapy for acute ischemic stroke is recombinant tissue plasminogen activator (rtPA), a systemic thrombolysis treatment (Marlier et al., 2015). For this drug to be effective, however, it has to be administered within 4.5h after symptoms first start. This small window results in rtPA being used in only 3-5% of stroke patients (Marlier et al., 2015).

An ideal stroke therapy would provide patients with some way in which to regain some, or all, of the function they lost due to a stroke. Towards this end, our group has set out to investigate the potential for using pulsed focused ultrasound (pFUS) to provide a safe, efficient, and minimally-invasive method for guiding neuroregenerative therapy in rat models. Our hypothesis is that pFUS treatment will result in an opening of the blood brain barrier while simultaneously triggering a localized increase in the release of stem cell recruitment cytokines like stromal cell-derived factor 1 (SDF-1). The opening of the blood brain barrier and the simultaneous release of chemoattractant cytokines, like SDF-1-alpha,

will increase the likelihood of transplanted umbilical cord blood stem cells homing to the targeted region of the brain. These results will support further investigation into the use of pFUS for endogenous, and exogenous, recruitment of neuroprogenitor stem cells.

## Background of the Problem

### *Generation of Neuroprogenitor Cells from Stem Cells*

Stem cells have been investigated as potential therapeutic agents, often with the purpose to restore a person's day-to-day functioning to normal, or baseline levels. Pathologies that have been investigated range from physically degenerative orthopaedic conditions, such as chondral defects, to genetically-defined neurodegenerative diseases like Hungtinton's disease (Gobbi et al., 2014; Olson et al., 2012). Indeed, stem cell replacement therapy for central nervous system disorders has shown promise. Cell types that have been used for this purpose include induced pluripotent stem cells (iPSCs), embryonic stem cells (ESCs), and mesynchymal stem cells (MSCs).

Descriptions of each of these cell types is provided by the National Institutes of Health and de Wert et al. (2003). In brief, embryonic stem cells are undifferentiated cells that are derived from preimplantation embryos that are capable of self renewal. They are also capable of dividing, without differentiating, into cells of the three primary germ layers: the ectoderm, mesoderm, and endoderm. Induced pluripotent stem cells are somatic cells that have been genetically transformed, due to the introduction of a number of embryonic genes,

such that they are also capable of self renewal and division into cells of the three primary germ layers. Mesenchymal stem cells are adult stem cells that come from many different tissue types, such as umbilical cord blood, and are capable of self renewal and can give rise to specialized cells.

Marlier et al. 2015 describes how embryonic stem cells and induced pluripotent stem cells have been used to create neuroprogenitor stem cells (NSCs) in order to investigate potential therapies for stroke. Neuroprogenitor stem cells are self-renewing, multipotent cells with the ability to give rise to neurons, astrocytes, and oligodendrocytes. A number of studies have investigated NSC transplantations in ischemic rat-brain models and have found migration of stem cells and significant functional improvements (Darsalia and Allison et al., 2011; Tajiri et al., 2014). Mesenchymal stem cells from umbilical cord blood are able to be directed to the neural lineage, and are also a viable alternative to embryonic stem cells (Bonaventura et al., 2015; Bużańska et al., 2006). Since different types of stem cells are capable of becoming NSCs, and because NSCs have the capacity to demonstrate functional improvements, it is important for the long term translational applicability of future neurorestorative investigations to weigh which source of stem cells would be most useful.

Dalous et al. 2012 describes how, of the various stem cell types used in research, human umbilical cord blood derived stem cells (hUCBSCs) have a number of advantages over the others. Since these stem cells are harvested from the blood of umbilical cords immediately after parturition, the collection of

cells from even a fraction of the 135 million births worldwide each year, means there would be potentially large amounts of cells that could be harvested. Another advantage is that harvesting itself poses no harm to the baby or mother, which would be a significant advantage over the aspiration of stem cells from bone marrow. This is also an advantage over the collection, and use, of more controversial stem cell types, such as embryonic stem cells (ESCs). Additionally, hUCBSCs are associated with a lower risk of viral contamination. Research on umbilical cord blood stem cells has shown that they have the potential to be used to regenerate cell types in the brain that are destroyed during the course of disease. With these advantages, hUCBSCs are worth investigating.

The blood brain barrier is a major obstacle to non-invasive, neuroprogenitor cell therapies. Studies have also demonstrated that neuroprogenitor cell implantations have a better success rate when directly injected into brain parenchyma as compared to intracerebroventricular injections or peripheral intravenous injections (Darsalia and Allison et al., 2011; Tajiri et al., 2014). While peripheral intravenous injections of NSCs has been shown to improve functional outcomes in models of acute ischemic stroke, the improvement was not linked to NSC migration into injured brain tissue and subsequent differentiation (Xiao et al., 2005). This was because few NSCs are found in brain parenchyma after peripheral injections (Xiao et al., 2005).

As Dadwalk et al. 2015 points out, endogenous stem cells have been shown to be able to proliferate and migrate to regions of injury to a limited degree

(Felling et al., 2006; Ong et al., 2005; Ikeda et al., 2005). The functional improvements demonstrated in models of acute ischemic stroke, appear to be due to the NSC induced downregulation of markers of inflammation, glial scar formation, and neuronal apoptotic death (Bacigaluppi et al., 2009). Inflammation may also play a role in attracting NSC's to areas of injury.

A couple of conclusions can be drawn from this research. One conclusion is that the lack of peripherally injected NSCs in the brain parenchyma could be due to a barrier of entry of some kind. The most likely culprit in this case would be the central nervous system's intrinsic mechanism of protection, the blood brain barrier. Another conclusion is that, if peripheral injections of NSCs were to be able to be pass through the blood brain barrier and home to the region of injury, as endogenous stem cells are able to do, the benefit in the acute stage may be a twofold: decreased inflammation in the area of the stroke and additional functional improvements from NSC differentiation and proliferation within the area of the stroke.

*Blood Brain Barrier*

The blood brain barrier (BBB) is a specialized, protective structure within the central nervous system. It is made up of microvascular endothelium, basement membrane, neurons, and support-type glial cells, including astrocytes, pericytes, and microglia (Winn et al., 2011). The blood brain barrier helps protect the central nervous system by selectively allowing only molecules with specific properties to cross into the brain. The selectivity of the blood brain barrier comes

primarily from the uniquely strong intercellular attachments that occur between capillary endothelial cells in the brain, called tight junctions (Kroll and Neuwelt, 1998). This is in contrast to the capillaries in the peripheral circulation, where endothelial cells are held together by much weaker intercellular attachments that more readily allow for paracellular transport (Abbott and Romero, 1996). In addition to the strength of the intercellular attachments between endothelial cells, transport across the blood brain barrier is limited due to the expression of specific efflux pumps on endothelial cells, the luminal negative charge of the endothelial cells, and the presence of supporting astrocytic podophilic projections (Abbott and Romero, 1996). Together, these limit penetrance into the brain based on three main filterable properties: lipid solubility, molecular size, and charge (Hynynen et al., 2001). This prevents ionized, water-soluble substances weighing greater than 180d from penetrating the blood brain barrier (Hynynen et al., 2001).

In limiting what can enter the central nervous system, the blood brain barrier becomes an obstacle to overcome when trying to deliver targeted therapies to the brain, as described by Jain et al., 2012. Compared to how easily drugs are able to pass from the plasma within the vasculature of other organs in the body, drug delivery to the brain is severely restricted. For instance, there is an 8-log difference between the rates of entry of small, lipid-soluble molecules compared to large proteins.

Work has been done to discover ways to circumvent the blood brain barrier in order to deliver therapies. The design of special delivery methods for drugs includes engineering them to be lipophilic, or taking advantage of amino acid and peptide properties, in order to use them as carriers capable of transporting the drug across the blood brain barrier (Hynynen et al., 2001). Clinically, blood brain barrier opening has been limited to the use of injections of hyperosmotic solutions, like mannitol (Hynynen et al., 2001). The injection of these solutions results in a transient fluid shift at the cellular level that causes the endothelial cells within the brain to decrease in volume. Typically lasting only for a few hours, this shrinking disrupts the tight junctions between endothelial cells, allowing for greater paracellular passage of substances (Blanchette et al., 2012). In these cases, the blood brain barrier opening occurs globally, however (Hynynen et al., 2001).

Clinically, focal opening of the blood brain barrier with hyperosmotic or chemical solutions has certain limitations. In order to achieve focal opening of the blood brain barrier this way there would have to be a direct injection to a specific region of the brain through a needle or catheter. Direct injections, however, carry the risk of neurologic damage, bleeding, and infection because they require opening of the skull (Hynynen et al., 2001).

Hynynen et al. 2001 and Jain et al. 2012 describe an ideal approach to opening of the blood brain barrier for delivery of therapeutic agents. They assert that in circumventing the blood brain barrier, the ideal method would be

anatomically localizable, readily controlled, transient, and non-destructive. The method should also be relatively selective for the therapeutic agent, and allow adequate concentrations of it to accumulate in the region of interest within the brain.

*Pulsed Focused Ultrasound*

Transcranial administration of pulsed focused ultrasound has the potential to be used clinically to circumvent the blood brain barrier when delivering a therapy. Pulsed focused ultrasound (pFUS) has been shown to meet the criteria Hynynen and Jain outlined for ideal approaches to blood brain barrier opening for delivery of therapeutic agents. It has been shown that pFUS can open the blood brain barrier in regionally targeted areas (Choi et al., 2007; Hynynen et al., 2001; McDannold et al., 2005; Vykhodtseva et al., 1995). This work used a variety of methods of testing for blood brain barrier opening, including magnetic resonance imaging and histological staining with trypan blue. It has also been shown that pFUS can be non-destructive, and transient, while focally opening the blood brain barrier (Choi et al., 2007; Hynynen et al., 2001, 2005; McDannold et al., 2004, 2005; Su et al., 2015).

Focused ultrasound can open the blood brain barrier through mechanical tissue disruption or by inducing tissue changes through focal temperature changes (Jang et al., 2010; Wrenn et al., 2012). The specific physics behind ultrasonic disruption of the blood brain barrier is beyond the scope of this paper, however, in brief, an appropriate summary on how pulsed focused ultrasound

produces its effects on tissue is provided by Jang et al. 2010. Here, Jang describes how ultrasound is a form of mechanical energy, much like how light is a form of electromagnetic energy. Similar to how light can be focused by a magnifying glass in order to concentrate enough energy within a small circumscribed area to elicit combustion, ultrasound energy can also be focused on a single circumscribed area. Then, by varying the acoustic properties (frequency, pulse length, pulse repetition frequency, and pressure amplitudes) of the waves targeted to a specific region, enough energy can be delivered to tissue to generate mechanical or thermal disruption at the molecular level.

*Mechanical disruption*

Multiple mechanical forces occur when tissue is exposed to focused ultrasound, each of which are thought to contribute to blood brain barrier disruption. These forces include acoustic cavitation, radiation force, shear stress and microstreaming (Fig i) (Jang et al., 2010; Liu et al., 2014). The most important of these forces to blood brain barrier disruption is acoustic cavitation, which occurs when a gas-filled bubble interacts with focused acoustic waves. These bubbles can form endogenously as a result of exposure to ultrasound fields with high peak negative pressures, or they can be exogenously introduced as a contrast agent via venous injection (Jang et al., 2010). Exposure of gas bubbles to ultrasonic waves results in mechanical oscillations, or changes in bubble size, in response to positive and negative pressures being delivered by the ultrasound field (Fig i – top) (Jang et al., 2010). Stable cavitation occurs when

bubbles expand and contract without reaching the critical point at which they would collapse (Liu et al., 2014). The expansion and collapse of these bubbles causes the movement of fluid around them, called microstreaming, which results in shear stress being applied to cell membranes. Inertial cavitation occurs when the bubbles are destroyed, or rapidly collapse. This results in additional forces that can act on tissue such as shock waves, microstreaming, and microjets (Fig 1) (Liu et al., 2014).

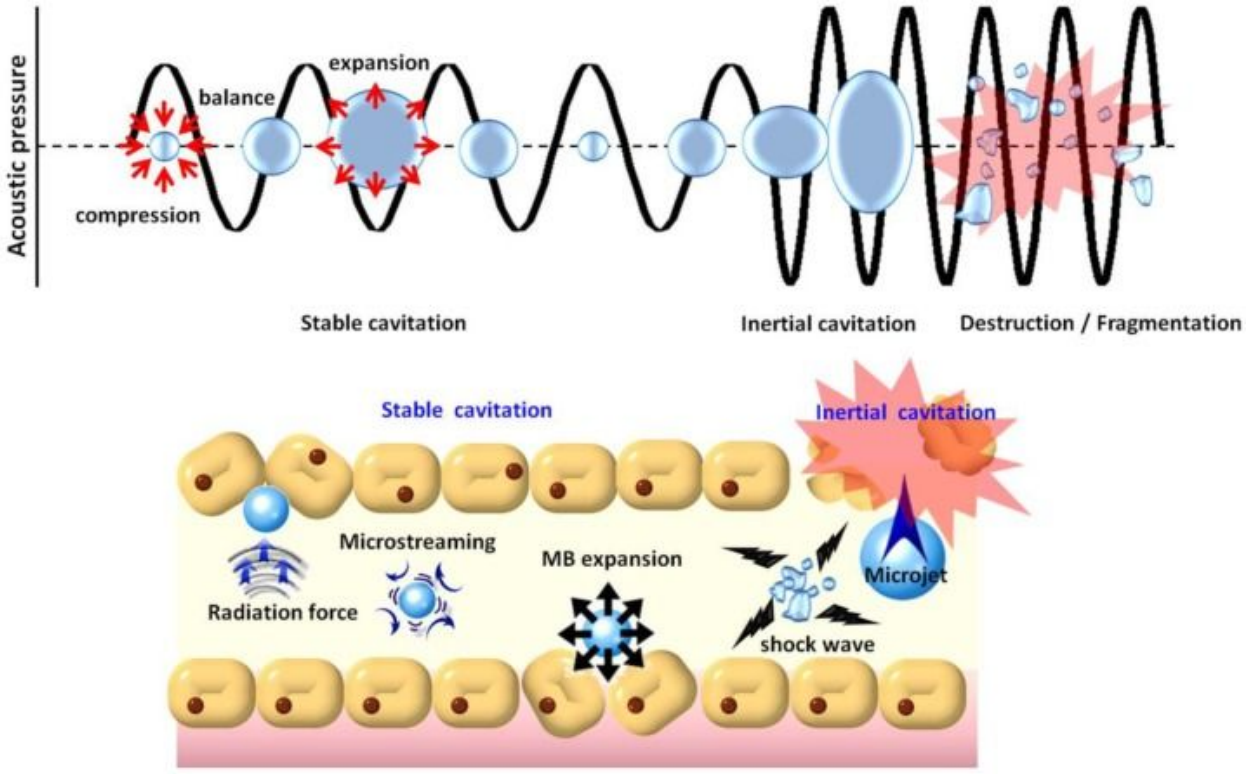


Figure i. Physical forces created by exposure of gas bubbles to ultrasound fields (Liu et al., 2014)

Microbubble contrast agents are engineered to improve focal disruption of the blood brain barrier and lower the risk of unintended tissue damage. The contrast agent generally used is lipid-encased and filled with perfluorocarbon or nitrogen

gas (Liu et al., 2014). These particular gases are used because of their low-diffusivity, and the lipid casing is intended to be made out of biodegradable material such as albumin, phospholipids, or polymers in order to limit toxicity (Liu et al., 2014). The administration of a contrast agent helps lower the threshold for blood brain barrier disruption. This allows delivery of relatively lower frequency ultrasound waves, which helps prevent tissue damage.

*Thermal disruption*

Focal temperature changes capable of opening the blood brain barrier result from absorption of ultrasound energy by tissue, and can be varied based on how the sonic energy is delivered (Jang et al., 2010). Focusing the ultrasound energy minimizes the potential for damage to tissue in between the transducer and the focal point because the energy delivered to this intervening tissue is significantly lower than at the focal point (Jang et al., 2010). The permeability of the interstitial epithelial tight junction barrier has been shown to vary in response to temperature increases within a physiologically relevant range (37-41°C) (Dokladny et al., 2006; Kiyatkin et al., 2009; Tabatabaei et al., 2015). Within this temperature range, the resultant blood brain barrier opening has also been shown to be reversible (Tabatabaei et al., 2015). This suggests that ultrasound used to generate focal temperature increases has the potential to result in transient blood brain barrier opening by affecting interstitial epithelial tight junctions.

*Stem Cell Homing to Tissue*

Pulsed focused ultrasound (pFUS) has been shown to guide stem cells to targeted organs, leading to functional improvements (Burks et al., 2013; Li et al., 2015; Tang et al., 2012; Wang et al 2016; Zhang et al., 2013). Signaling pathways activated by targeted pulsed focused (pFUS) ultrasound treatment of tissue have been demonstrated to be important for the homing of mesenchymal stem cells (MSC) to targeted regions (Nguyen et al., 2015; Tebebi et al., 2015). Specifically, the signaling mechanism thought to be involved in MSC homing, is a result of how mechanical disruption of tissue by pFUS establishes a gradient of local cytokines, chemokines, and trophic factors in the targeted region (Tebebi et al., 2015). A signaling molecule that is released in response to neurological injury and participates in endogenous stem cell recruitment is stromal cell-derived factor 1 (SDF-1) (Imitola et al. 2004, Xue et al., 2015). It is believed that this effect is largely a result of SDF-1, also known as chemokine ligand 12 (CXCL12), binding to the receptor known as chemokine receptor 4 (CXCR4) (Xue et al., 2015). Evidence of sonic waves increasing release of SDF-1 within the spinal cord was demonstrated by Lee et al., 2014. Evidence has also shown that increased levels of SDF-1 in the brain can lead to stem cell recruitment (Li et al., 2015). Therefore, it is possible that ultrasonic treatment of the brain could result in increased expression of SDF-1, which in turn could lead to stem cell recruitment to targeted regions of the brain.

**Summary of Unresolved Issues and the Significance of the Study**

There is a significant gap in our knowledge when it comes to clinical therapies for stroke. One approved therapy for stroke, that can only be administered within a narrow window of time after symptoms occur, is inadequate. Therapeutic promise has been demonstrated by neuroprogenitor stem cell investigations, but specific research into the use of umbilical cord blood stem cells for treatment of stroke is lacking in regards to adjuvant therapy with pulsed focused ultrasound. This is an important avenue of investigation, as it provides the opportunity to pursue therapy that addresses the major obstacle to minimally invasive peripheral injections of UCBSCs, the blood brain barrier. Not only does ultrasound demonstrate the potential to overcome this physical barrier, but ultrasound may simultaneously address an additional delivery concern, stem cell homing to the area of injury in patients with chronic stroke. The capacity to assist with cellular homing would make this a viable therapy, not only in the acute stroke patient, but also those who have lived with disability for years.

**Purpose of the Study**

The purpose of my work will be to (1) quantitatively demonstrate blood brain barrier opening with pulsed focused ultrasound treatment of Sprague Dawley rats using Evans Blue vs control; (2) assess the safety of ultrasonic therapy energy levels on rat brain tissue using histologic analysis of TUNEL markers; (3) quantitatively demonstrate CXCL12 upregulation in ultrasound treated rat brain tissue vs control; quantitatively demonstrate CXCL12:CXCR4 coexpression levels in ultrasound treated rat brain vs control; and finally, (4)

quantitatively identify CXCL12:CXCR4 expression by different cell types, including astrocytes, microglia, oligodendroglia, and neurons.

**Assumptions, Limitations, and Scope (delimitations)**

- I will be limited by the number of rats that will be ultrasonically treated and the amount of experimental brain tissue available to analyze.
- This research is on rats, and rats have a significantly thinner skull than humans. As a result, even promising results may not be translatable to human studies until the obstacle of targeting ultrasonic waves through the human calvarium is resolved.

# Materials and Methods

*Pulsed focused ultrasound experiments*

The head of the rat was shaved to reduce interference with the sonic waves. We also shaved the right side of the rat to be able to place leads that could be used to monitor the rat's vital signs during the procedure. The rat was then anesthetized and laid on a heating pad in the prone position under the ultrasound probe. Leads were attached to monitor the rat's body temperature, heart rate, and breathing rate throughout the procedure. The rat's head was stabilized bilaterally with two ear rods to improve accuracy. The ultrasound device was lowered into place atop the rat's head and the posterior, and middle, aspect of the cerebellum was identified. Movement of the ultrasound device was measured from this point. A total of 4-5 pulses were delivered to each half of the brain (cerebellum and cerebrum). Measurements of the temperature in the targeted region, and within the surrounding tissue, were taken with each pulse treatment (method described elsewhere in Haritonova et al., 2015). The amount of energy delivered with each pulse and the number of pulses was recorded.

*Evans Blue Dye Injections*

A cohort of 5 rats was injected with Evans Blue Dye (4 mg/kg of a 2% solution dissolved in normal saline) 20 hours after the ultrasound treatment to assess for blood brain barrier opening. Research Animal Resources (RAR) staff performed the tail vein injections. These animals were sacrificed 25 minutes after the Evans Blue Dye injection, in accordance with the approved protocol, using a

lethal dose of CO2. Death was confirmed using the toe pinch, tail pinch, and corneal reflex methods.

*Perfusion*

After sacrifice, all rats were then perfused. To begin the procedure for the perfusion, the rat was laid supine on an absorbent blue pad. Using gloved hands, the xyphoid process was identified at the midline of the chest. Using toothed tweezers, the skin lying atop the xyphoid process was lifted to elevate the abdominal wall away from the abdominal contents, and an incision through the abdominal wall was made immediately caudal to the xyphoid process. The incision was extended bilaterally with scissors by cutting along the caudal edge of the ribcage towards the midaxillary line. Next, the diaphragm was dissected away from its insertion to the ribcage, beginning at the midline and extending bilaterally towards the midaxillary line. The ribcage was cut along the midclavicular line from about the seventh rib to the clavicle. The anterior chest wall was then carefully reflected 180° as the fat strands attaching the heart to the anterior chest wall were dissected away from the thoracic wall. A hemostat was used to hold the anterior chest wall in place against the anterior aspect of the subject's neck.

To begin the perfusion, 60mL of PBS was drawn up into a 60 mL syringe. The syringe was attached to one end of a 45cm length of peripheral IV (PIV) tubing with a 26 gauge perfusion needle attached to the other end. The left and right ventricles and atria of the heart were identified, and the needle was inserted

into the left ventricle of the subject's heart to ensure adequate perfusion of the systemic circulatory system with PBS. A small cut was made in the right atrium, which would allow the blood to drain while permitting the PBS the chance to pass through the majority of the subject's circulatory system. About 90 mL of PBS was required before clear fluid began to drain from the subject's right atrium, a sign that enough blood had been flushed from the rat's circulatory system to allow for adequate preservation of tissue. At this point, 60 mL of 4% PFA was drawn up into the syringe and injected into the left ventricle of the rat. At least 90 mL of 4% PFA was injected before signs of adequate perfusion were observed: stiffness in the extremities and immobility of the neck when subject is gently lifted from surgical field. At this point the perfusion needle was removed, the hemostat unclamped, and the blue absorbent pad removed from the surgical field and replaced with a fresh one.

*Brain tissue collection*

In each case, the skin covering the dorsal and lateral aspects of the neck of the subject were dissected away from the muscles of the neck to allow for easier access to the skull. The skin on the anterior aspect of the neck was left intact to make handling of the skull and dissection of tissue easier. Using a sharp iris scissor and ronger, muscle and connective tissue was dissected away from the posterior skull, exposing the parietal and occipital bones as well as the foramen magnum. Next, the tissue in between the foramen magnum and the anterior hard palate was dissected away to expose the inferior skull. On either

side of the skull, the lateral tympanic bullae were removed. The zygomatic arches were broken at their insertion near the squamosal bone and the lower jaw was dissected away bilaterally.

To access the brain once the majority of the skull had been exposed, the occipital bone was removed by entering the foramen magnum with a small ronger or tweezers and extending the opening superiorly and laterally. Next, using the same tools, the postero-inferior bones of the subject's skull were dissected away to expose the brainstem, inferior cerebellum, and inferior temporal lobes. Bones inferior to the temporal crest, from the lamboidal crest to midway through the frontal bone, were dissected away from the lateral skull to expose either side of the cerebrum, cerebellum, and brainstem. At the same time, continuing from caudal to rostral, the remaining bone that covered the brain inferiorly was dissected so that the anterior frontal lobes, and inferior olfactory nerves, could be visualized. The olfactory nerves were dissected away from the cribriform plate to allow the brain to be removed, intact, from the remaining skull. From posterior to anterior, the brain was carefully dissected away from the remaining interparietal, parietal, and frontal bones, and lifted out of the skull.

*PFA saturation and preparation for cryopreservation*

Once removed from the skull, the brain was placed in 50 mL of 4% PFA, within a 50 mL Falcon tube. Since the brain was still intact at this point, it was kept at room temperature for 24 hours in 4% PFA to allow for adequate tissue saturation. The following day the brain was transferred into a 30% sucrose

solution to help protect the tissue from damage during the freezing process. It was then stored for 24 hours at 4°C overnight.

*Evans Blue dye visualization*

The brains of the rats that had received the Evans Blue dye injections were removed from the 30% sucrose solution at 24 hours and placed, with the superior aspect facing up, in a brain mold to allow for cutting of the tissue into 1-3mm sections. A razor blade was placed at the front of brain, taking into account the length of the cerebrum, so that it wasjust touching the anterior frontal lobes. A second razor blade was placed between the cerebrum and cerebellum, and a third just touching the posterior cerebellum. One at a time, additional razors were added to the mold so that the brain was separated into 1-2 mm sections. These sections were then moved to a petri dish and aligned in a row, with the posterior (caudal) aspect of each section resting against the bottom of the dish. The scanner was then prepared, and these sections were moved onto the scanner and placed in the same manner, aligned in a row so that the posterior (caudal) aspect of each section was resting against glass of the scanner. A ruler was placed next to the tissue to demonstrate size, and a note on the orientation of the tissue was placed adjacent to this to later help identify orientation. The same was done with the anterior (rostral) side resting against the glass of the scanner.

The tissue was then moved into a 12 well plate. Next, a round glass slide was placed in each well to help ensure the tissue maintained its orientation while

in the well. About 2.5 mL of a 30% solution of sucrose was added to each well. The labeled plate was moved to freezer and stored at 4°C.

*Cryopreservation of wild type rats and pFUS+/EB- Rats*

To demonstrate a normal phenotype, rats brains not treated with ultrasound were used as a control. To ensure the integrity of the normal phenotype, these rats were not injected with Evans Blue Dye. These control brains were compared against tissue that had been collected from pFUS treated rats that had not been injected with Evans Blue dye (EB-). This was to reduce confounding variables. The following procedure for cryopreservation applied to both control brains and pFUS treated rat brains that had not been exposed to Evans Blue dye.

The brains of the wild type and pFUS+/EB- rats were removed from a 30% sucrose solution after 24 hours in the solution. In order to help with identification of brain regions that would later be visualized with immunohistochemistry, the brain was cut, using a razor blade into 7 pieces. First, the brain was placed, with the superior aspect facing up, on a petri dish, and the cerebrum was separated from the cerebellum. The cerebrum was then cut in half along the midline. The medial aspect of each cerebrum was then moved close to the edge of the petri dish so that landmarks could be visualized. One coronal cut was made along the anterior edge of the genu of the corpus callosum, and a second cut was made at the posterior edge of the splenium of the corpus callosum. Each of the seven brain sections was then placed into individually labeled molds. The molds were

then slowly filled with OCT so that the top of the brain sections were about 4 mm from the surface of the OCT. The molds were then placed in an insulated container that contained dry ice. They were left in the box until the OCT appeared completely frozen, about 5-10 minutes. The sections were then wrapped in tinfoil and placed in a cryopreservation bag within a labeled box for freezer storage. The tissue was then stored in the box at -80°C.

*Cryosectioning*

A cryostat was used to section rat brain tissue. Frozen brain tissue was sectioned at 10 microns. After sectioning, the slides were stored in a freezer at -80°C.

*Antigen retrieval*

After removing slides from -20°C freezer storage, and allowing them to dry and come to room temperature for at least 15 minutes, antigen retrieval using a citrate buffer and vegetable steamer was performed. This step was intended to improve staining by breaking some of the protein cross-linking bonds formed during the fixation process in order to uncover otherwise inaccessible antigenic sites. The following protocol is based on what was recommended by Abcam.

With the slides warmed to room temperature, the vegetable steamer was set up. Then, the buffer (10mM sodium citrate, 0.05% Tween 20, pH 6) buffer was added to the rack of slides, and that rack of slides was placed in a lidded container within the vegetable steamer. The buffer solution was heated in the vegetable steamer until its temperature was 95°C. The slides were then carefully

placed in the racks, with the non-labeled end immersed in the buffer. A second slide was gently placed over the first to allow the citrate to be drawn up across the tissue, without the risk of the tissue falling off the slide. The lid to the rack container and the steamer were closed, and the slides were left to incubate in the vegetable steamer for 30 minutes. Afterwards, the slides were allowed to cool back down to room temperature for 30 minutes before moving on.

*Immunohistochemistry*

The following protocol is based on recommendations made by Abcam. A barrier was created around the tissue using a PAP pen to keep solutions from running off slides. Next, a second barrier was created on each slide between the negative control tissue and the experimental tissue. The slides were then washed twice (0.025% Triton X100 in PBS) for five minutes to gently permeabilize the tissue and make the antigens more accessible. A block solution (10% normal serum with 1% BSA in PBS) was applied to prevent background staining. With the block applied, the slides were kept in a humidified slide box with wet paper towels for an hour. The slides were drained and a control solution (PBS with 1% BSA) was applied to the control tissue. The primary antibodies, in solution with 1% BSA in PBS, were then applied to the experimental tissue and stored in a humidified slide box, at 4°C, overnight.

The next day, the slides were removed from the 4°C cooler and washed twice (0.025% Triton X100 in PBS) to permeabilize the cells membranes and to create better access to the primary antibody epitopes. The

fluorophore-conjugated secondary antibodies (diluted in a 1% BSA solution in PBS) were then applied to both the experimental tissue and the control tissue. The slides were kept in a humidified slide box, with wet paper towels, for 1 hour. Afterwards, the slides were washed three times in PBS for 5 minutes. The slides were then stained with DAPI (1:1000 in PBS) to help visualize the location of the cells in the tissue. The slides were washed twice in PBS for 5 minutes, and then mounted by applying Immuno Mount to the slides, covering them with glass coverslips, allowing them to dry for 10 minutes, and sealing the glass slides and coverslips with clear nail polish remover. The slides were moved to a slide box and placed in a freezer at -20°C.

# Results

### Nestin and Doublecortin Staining

Staining was done on control, Sprague Dawley, rats in order to develop an appropriate technique capable of visualizing the antigens of interest. Our first antigens of interest, nestin and doublecortin, were used in order to visualize endogenous stem cell populations.

Sections of left striatum were stained with a primary antibody targeting Nestin (EMD Millipore, Chemicon Brand, MAB 353, mouse-anti-nestin), at a concentration of 1:500, and counterstained with DAPI. Per the manufacturer's description, Nestin is a large intermediate filament that is expressed primarily by central nervous system stem cells in the neural tube, and is thought to be a reasonable neuronal marker. Initial results demonstrated what appeared to be a mild amount of background staining, but neurons appeared to be appropriately labeled in the region of the hippocampus (fig. 1 D-I). There was also staining of cortical neurons (fig.1 D-F), and subventricular zone neurons (fig. 1 J-L).

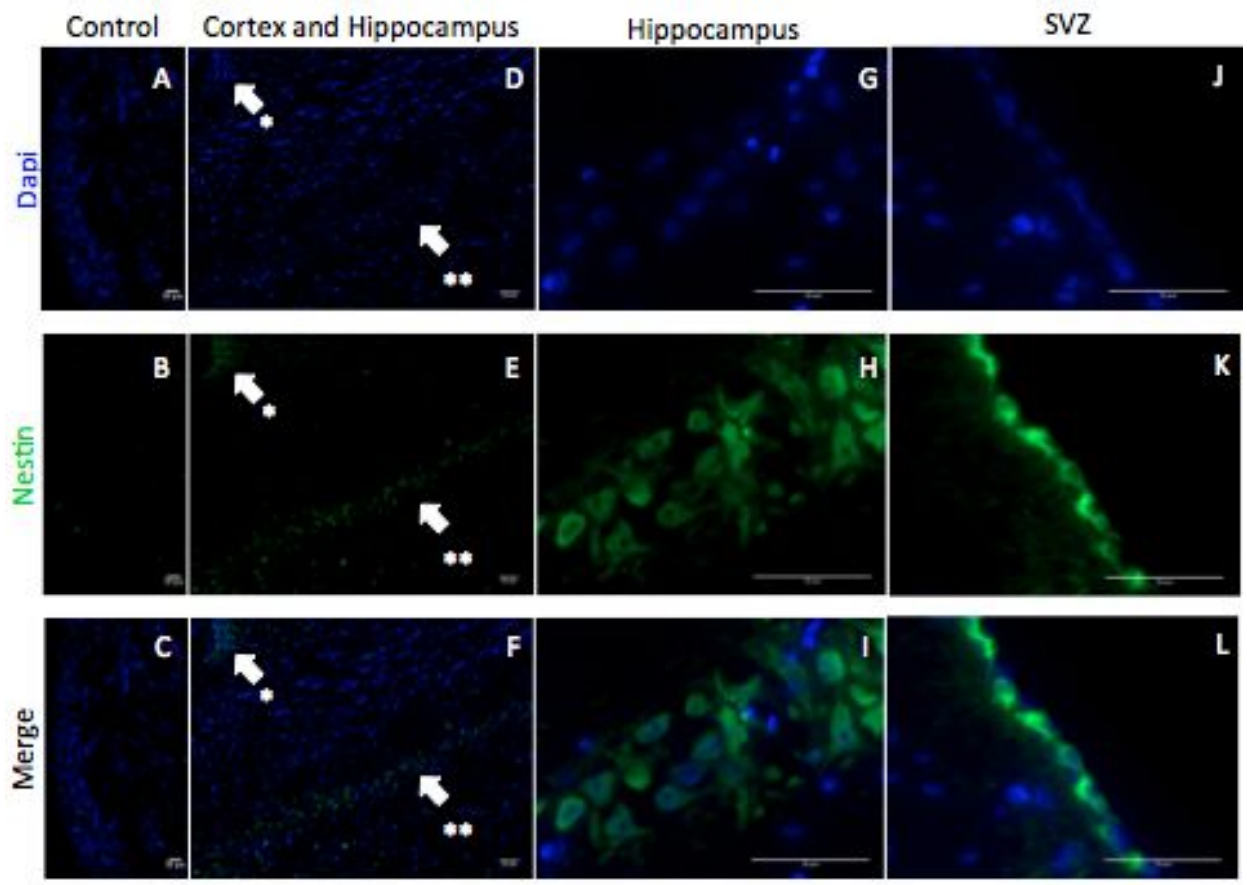


Figure 1. Coronal sections of wild type Sprague Dawley rats, Nestin (green) and counterstain DAPI (blue), 50μm scale. (A-C) Control samples. (D-F) cerebral cortex (*) and hippocampal dentate gyrus (**). (G-I) Dentate gyrus cells within hippocampus. (J-L) Subventricular zone (SVZ), with ventricle on right.

Similarly, sections of left striatum were stained with a primary antibody targeting doublecortin (Santa Cruz Biotechnology, Inc., sc-8067 (N-19), goat-anti-doublecortin), at a concentration of 1:100, and counterstained with DAPI. Brown et al. 2003, describes doublecortin as a microtubule binding protein that is associated with neuroblast migration, and demonstrates how it could be used as a marker to detect neurogenesis in the adult mammalian brain. In adult mammalian brains, it has been shown to be expressed in the dentate gyrus and

subventricular zone, but my attempts to visualize doublecortin within these regions failed (results not shown). With each attempt there appeared to be a significant amount of background staining, and positive staining could not be demonstrated.

**CD11b/c, Iba1, Calbindin, Myelin Basic Protein, GFAP, Neurofilament 68 staining**

Staining was done on control, Sprague Dawley, rats in order to develop an appropriate technique capable of visualizing the antigens of cell populations likely to be affected by pulsed focused ultrasound therapy.

Microglia are support cells in the brain that are immunologically active and play a role in neurogenesis within the ventricular-subventricular zone (V-SVZ) (Fonseca et al., 2016). Fonseca et al. 2016, describes how, after an injury of infection, these cells become activated. Depending on the activation state, microglia can have positive or negative influence on neurogenesis (Butovsky et al., 2006). If endogenous chemokines, like SDF-1, were to be released as a result of pulsed focused ultrasound (pFUS), it is likely that microglia would be activated. This would make them an important cell population to observe in relation to neural stem cell (NSC) activity and pulsed focused ultrasound treatment.

Microglia in the brain can be visualized by targeting intracellular and extracellular antigens. The cell surface marker, called cluster of differentiation marker 11b/c (CD11b/c), was targeted in our experiments in order to visualize

microglia. Microglia can also be visualized using antibodies targeting ionized calcium binding adaptor molecule 1 (Iba1). This intracellular molecule has an actin-bundling activity that assists microglia in the process of membrane ruffling and phagocytosis in activated microglia (Ohsawa et al., 2004). Together, then, antibodies targeting these antigens can be used to not only look for the presence of microglia, but also the relative activation status of microglia as well.

Initial staining with CD11b/c was begun at 1:50 (Abcam, mouse anti-CD11b/c, [OX42]). Using imaging to visualize the staining, CD11b/c cells were able to be visualized throughout the brain (fig. 2 A-C). Upon closer inspection of the hippocampus, CD11b/c staining was visualized well throughout (fig 3. A-C, G-I). Initial staining with Iba1 (Abcam, mouse anti-Iba1, ab15690) was begun at 1:100. Microglia weren't visualized at this concentration (results not shown). With the strong results of the CD11b/c, additional titration of CD11b/c was pursued over Iba1 at this time.

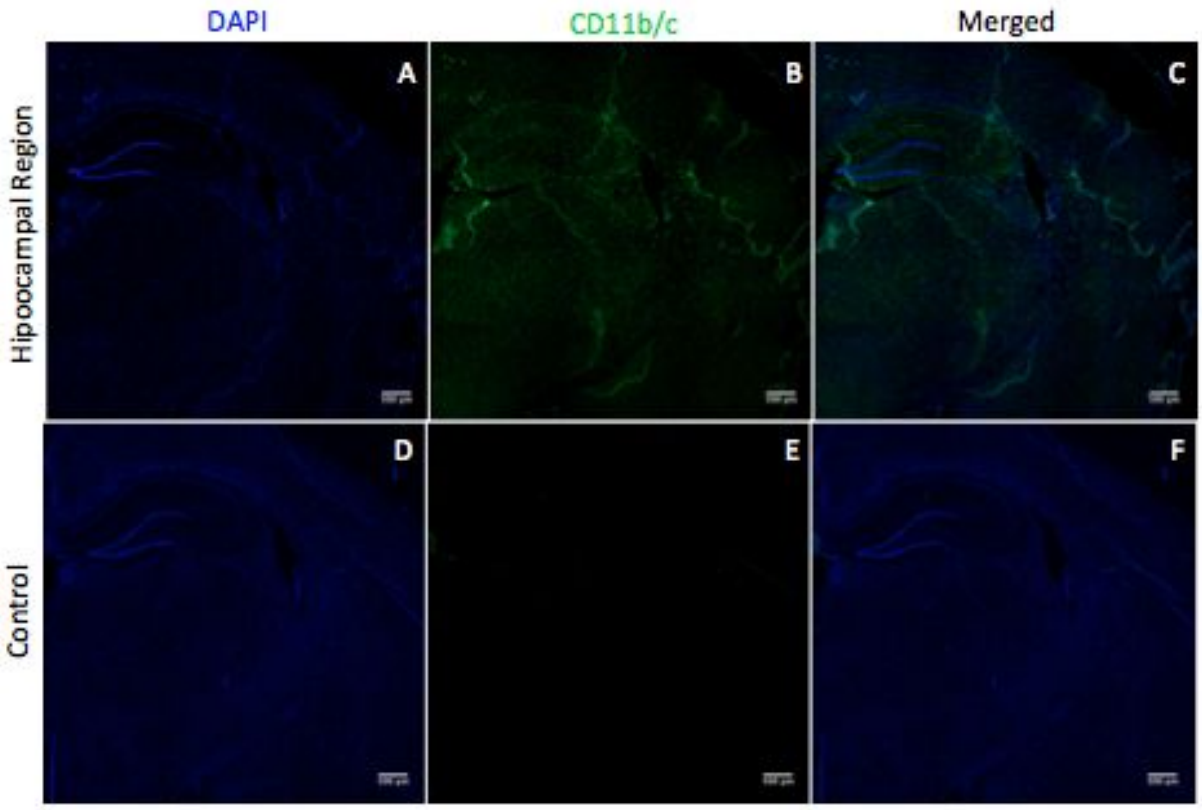


Figure 2. Coronal sections of wild type Sprague Dawley rats, CD11b/c (green) and counterstain DAPI (blue), 500μm scale. (A-C) Visualization of hippocampus as well as subventricular zone (SVZ), large portions of the cortex, and deep structures. (D-F) Control tissue visualizing same regions.

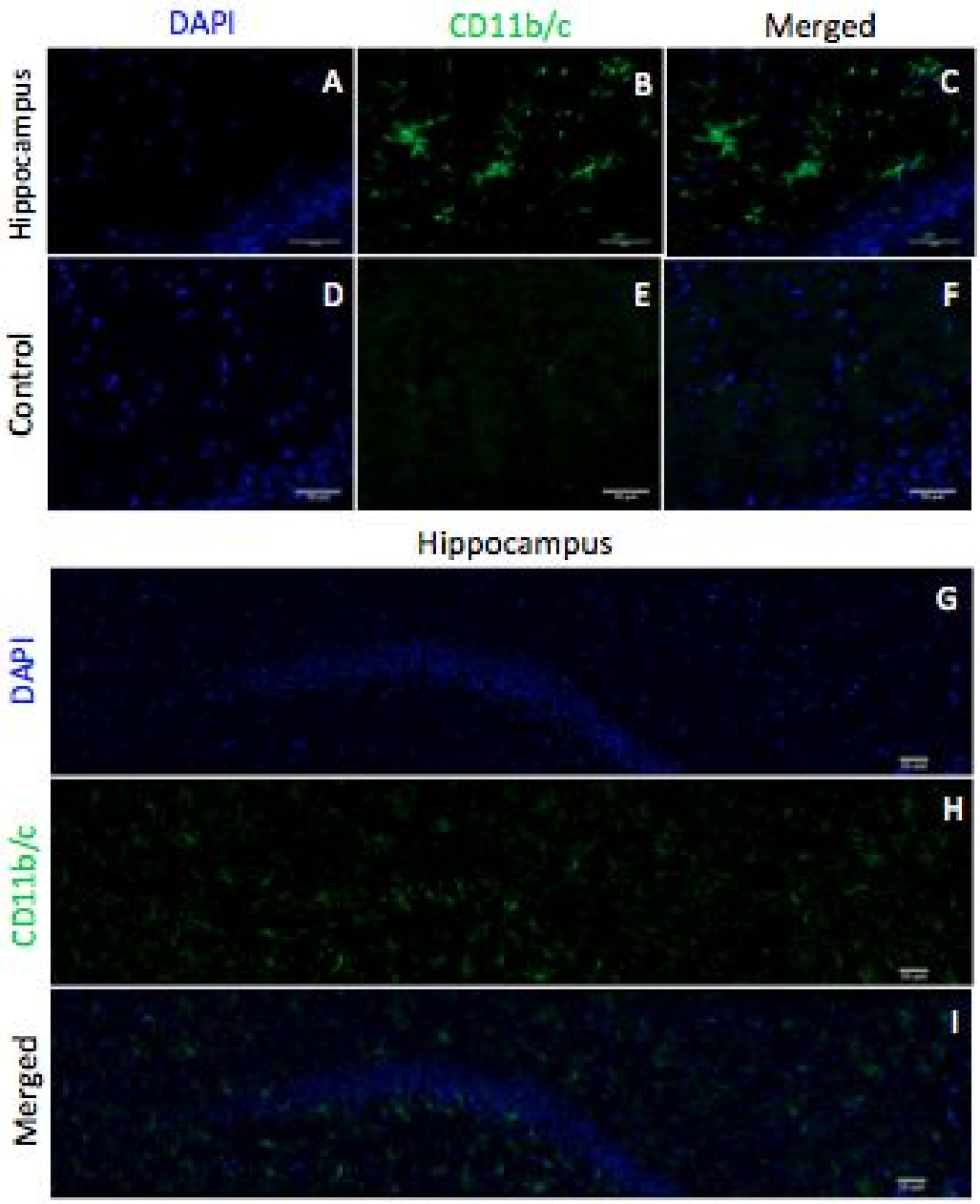


Figure 3. Coronal sections of wild type Sprague Dawley rats, CD11b/c (green) and counterstain DAPI (blue), 50μm scale. (A-C) Visualization of dentate gyrus cells within the hippocampus. (D-F) Control tissue visualizing same regions. (G-H) Larger field of view of hippocampus and dentate gyrus.

Calbindin-D28K is an intracellular calcium-buffering protein that can be found within specific subpopulations of inhibitory GABAergic interneurons. Calbindin functions to maintain homeostatic concentrations of neuronal intracellular calcium. Within the hippocampus, a region of the brain demonstrated to maintain subpopulations of endogenous neural stem cells (Gage et al., 1998; Lois et al. 1993; Patel et al., 2016), Verdeguer et al., 2015 has demonstrated that this protein may play a role in influencing and maintaining adult neurogenesis. Therefore, investigating how calbindin expression is influenced by pulsed focused ultrasound could demonstrate significant insight into cellular mechanisms behind the stimulation of neurogenesis in the adult brain.

In order to observe the effects pulsed focused ultrasound may have on homeostatic neurogenesis, initial staining on control rat brain sections was performed with calbindin (Swant, CB-28a, rabbit anti-calbindin-D28K) at 1:500 and CD11b/c (Abcam, mouse anti-CD11b/c, [OX42]) at 1:500. Initial attempts at staining were unable to produce positive imaging results of calbindin (results not shown).

Oligodendrocytes in the central nervous system synthesize lipids and proteins to form sheets of cellular membrane material called myelin. Myelin wraps around axons in discrete multilayered stacks and functions to insulate nerves. In doing so, myelin allows nerves to propagate action potentials via saltatory conduction. This fundamental physiological process within the central

nervous system (CNS) allows for the rapid processing of information in a relatively small space (Aggarwal et al., 2011). Consequently, as noted by Li et al., 2015, remyelination is an important repair process after an ischemic injury.

Myelin basic protein (MBP) is the most abundant extrinsic myelin membrane protein (Deber et al., 1991). Visualizing this protein, then, provides information on the presence of myelin. Determining the presence of myelin after an ischemic injury would be useful because myelin is required for healthy processing and signaling within the CNS. The relative abundance of myelin in a region of ischemic brain would be useful to observe, because greater than expected concentrations of myelin in the ischemic regions after treatment with pfUS would support the need for additional studies that would demonstrate restoration of damaged tissue.

Towards this end, we set out to stain for myelin basic protein (Sigma Life Sciences, M3821, rabbit anti-MBP) at initial concentrations of 1:100. Sections were costained with CD11b/c (Abcam, mouse anti-CD11b/c, [OX42]) at 1:500. Looking at both of these antigens at the same time was thought to be useful in that it may show a relationship between microglial populations and the presence of myelin. Initial attempts at staining were unable to produce positive imaging results of MBP (results not shown).

The presence of neurons was investigated by staining for neurofilament 68. Neurofilaments are intermediate filaments with a diameter of 10nm, and are particularly abundant in neuronal axons. Neurofilament 68 (NF-68) is a specific

antigenic subtype that weighs 68 kD (Yuan et al., 2012). Our interest in staining for the neurofilament 68 (Sigma-Aldrich, N5139, monoclonal mouse anti-neurofilament 68, clone NR4) antigen was to be able to visualize the impact of pFUS on the neuronal cell population. Initial stains were conducted at concentrations of 1:500. These sections were also costained with antibodies targeting glial acidic fibrillary protein (GFAP) (Dako, polyclonal rabbit anti-GFAP, Z0334) at a concentration of 1:100. Glial acidic fibrillary protein is an antigen found on reactive astrocytes. Astrocytes are specialized CNS support cells that are over five times more abundant than neurons. These cells line the CNS, and respond to CNS insults through a process called reactive astrogliosis (Sofroniew et al., 2010). Understanding how astrocytes may be affected by pulsed focused ultrasound treatment of ischemic brain tissue could help illuminate mechanisms behind its potential therapeutic effects. Initial attempts at staining produced poor imaging results of GFAP and Neurofilament 68 (results not shown).

**Ki-67 staining**

Additional staining was done on control, Sprague Dawley, rats in order to develop an appropriate staining technique capable of visualizing cellular proliferation. The antibody chosen for this purpose targets an intranuclear proliferation antigen, designated Ki-67. Johannessen et al., 2006, describes how the Ki-67 antigen is present in proliferating cells but not in quiescent cells. While the precise function of the Ki-67 protein is unclear, it is known to be present in all phases of the cell cycle, except G0 and the early part of G1, making a good

marker of cellular division. Tissue sections were initially costained with Ki-67 (Leica Biosystems Novacastra™ lyophilized rabbit anti Ki-67 polyclonal antibody, NCL-Ki67p) at 1:1000 and Nestin (EMD Millipore, Chemicon Brand, MAB 353, mouse-anti-nestin) at 1:100. In visualizing the results, good staining with Ki-67 was demonstrated, with some co-staining of Nestin evident (fig. 4 E-P). It also appeared that Ki-67 stained cells that appeared not to be positive for Nestin (fig. 4 H, L, P).

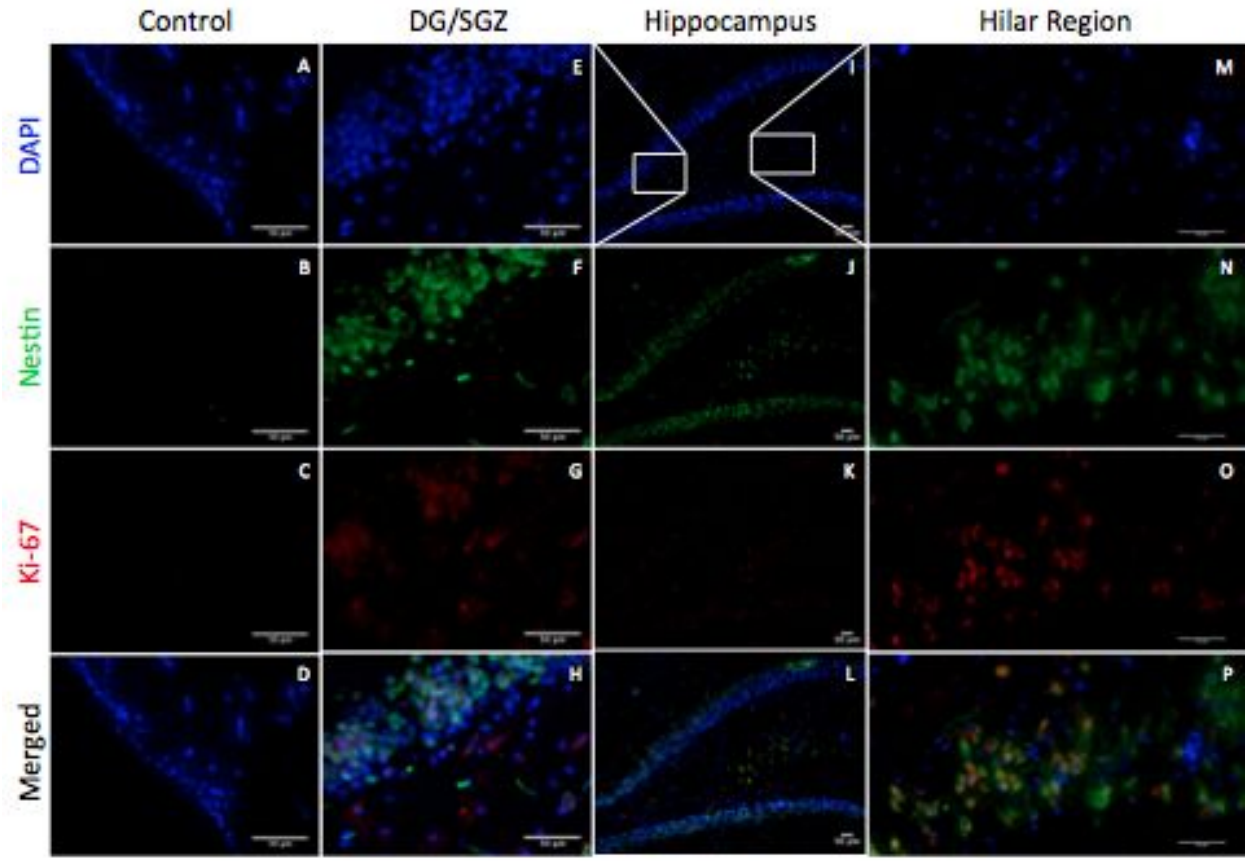


Figure 4. Coronal sections of wild type Sprague Dawley rats, Nestin (green), Ki-67 (red) and counterstain DAPI (blue), 50μm scale. (A-C) Control tissue. (E-H) Visualization of dentate gyrus cells and subgranular zone (SGZ) cells within the hippocampus. (I-L) Hippocampus tissue. (M-P) Hilar region (HR) of hippocampus.

**SDF-1 and CXCR4 staining**

Additional staining was done on control, Sprague Dawley, rats in order to develop an appropriate staining technique capable of visualizing stem cell recruitment cytokines and their receptors. The stem cell recruitment cytokine of interest we targeted

Stromal cell-derived factor 1 (SDF-1), also called c-x-c motif ligand 12 (CXCL-12), and its receptor, c-x-c motif receptor 4 (CXCR4), have been demonstrated to be important in stem cell recruitment and homing (Lapidot et al., 2002). Li et al., 2015, demonstrated that there could be a therapeutic benefit to taking advantage of this role of SDF-1. In their experiment, they demonstrated that the transduction of the CXCL-12 gene into murine brain tissue near ischemic brain regions resulted in white matter repair after ischemic injury. They demonstrated that this was likely due to resultant oligodendroglial progenitor cell proliferation and differentiation. If pulsed focused ultrasound therapy of injured brain tissue could be shown to increase SDF-1 expression, similar repair of tissue injured by ischemia may result.

In order to observe colocalization of SDF-1 and CXCR-4, rat brain sections were stained with antibodies targeting SDF-1 (Abcam, polyclonal rabbit anti-SDF-1, ab25117) at concentrations of 1:100 and CXCR-4 (Abcam, polyclonal goat anti-CXCR-4, ab1671) at concentrations of 1:100. Subsequent concentrations that were used were 1:150, 1:200, and 1:300. Initial results demonstrated apparent costaining of CXCR-4 and SDF-1, with possible

differences in degree of costaining depending on the region of the brain: subcortical, cortical, subventricular (fig 5. E-P). A progressively increasing amount of costaining appeared to be demonstrated with progression from cortical to deeper structures of the brain.

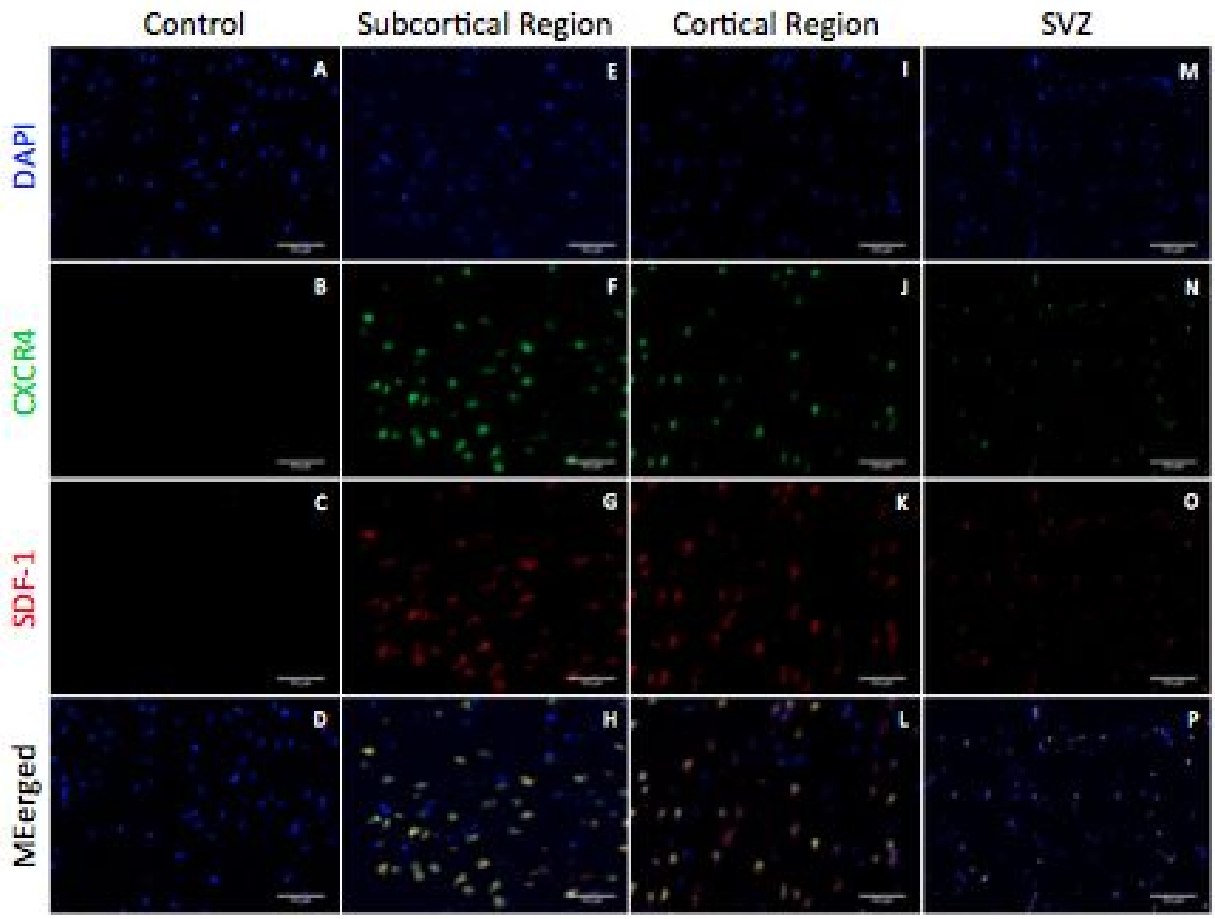


Figure 5. Coronal sections of wild type Sprague Dawley rats, CXCR4 (green), SDF-1 (red) and counterstain DAPI (blue), 50μm scale. (A-C) Control tissue. (E-H) Visualization of subcortical regions of brain. (I-L) Deeper cortical tissue. (M-P) Subventricular zone (SVZ) tissue.

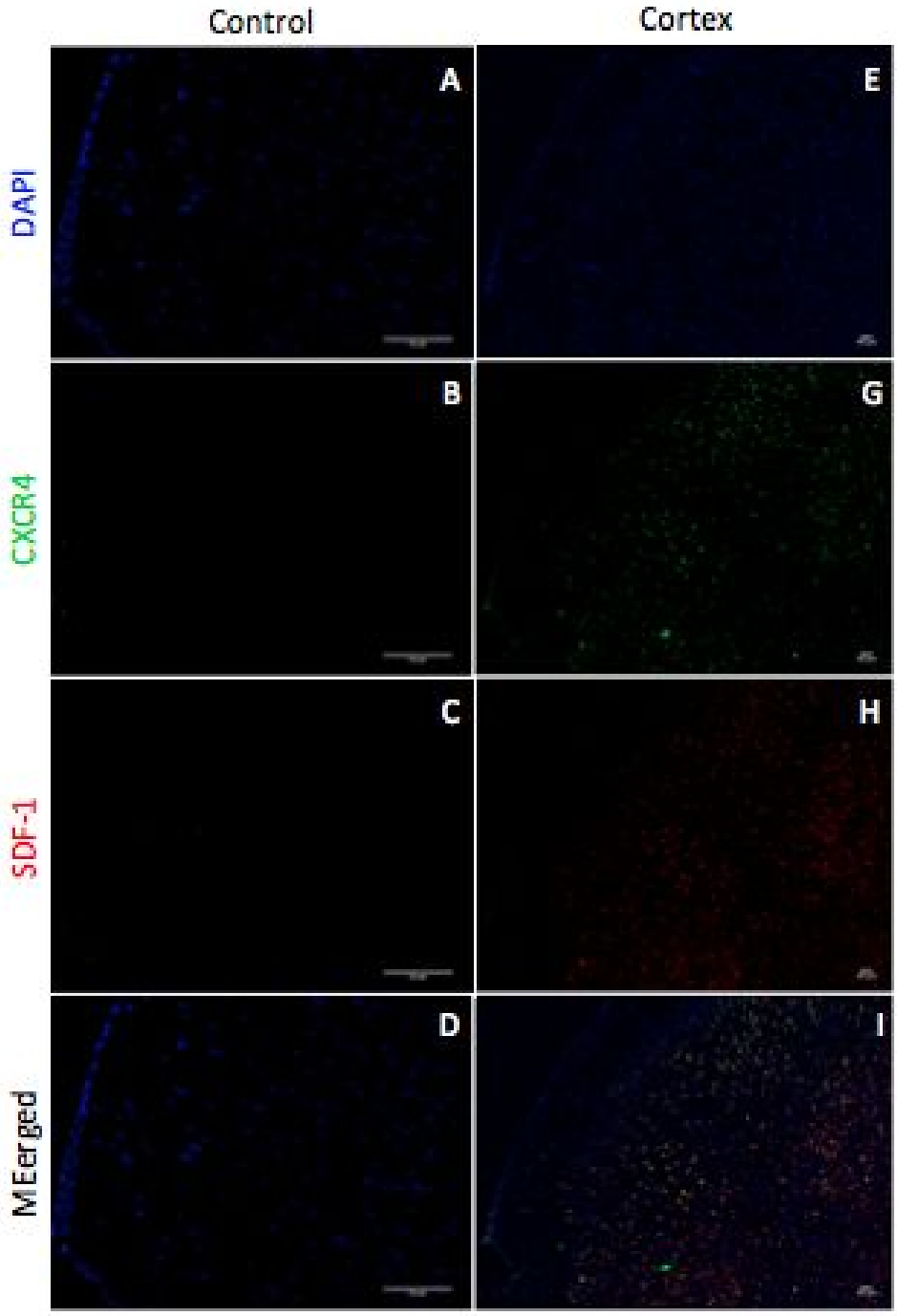


Figure 6. Coronal sections of wild type Sprague Dawley rats, CXCR4 (green), SDF-1 (red) and counterstain DAPI (blue), 50μm scale. (A-D) Control tissue. (E-I) Visualization of cortical regions of brain (cortex in upper left of field) and some deeper structures (bottom right).

**Evans Blue Staining**

Evans Blue experiments demonstrated evidence of likely blood brain barrier opening as a result of pulsed focused ultrasound treatment of rat brain tissue. Evans Blue dye is commonly used in experiments that investigate blood brain barrier opening. It is used because it binds to albumin, and is only capable of staining brain tissue if the blood brain barrier is compromised (Leinenga et al., 2015). In our pFUS, experiments, then, we would expect that if the blood brain barrier was opened, albumin, as well as the dye, would extravasate into brain tissue. This would result in blue-stained brain tissue where the blood brain barrier was opened.

Evans Blue dye staining was first assessed with serial cryostat sectioning and imaging. In this experiment, a rat brain treated with Evans Blue dye was perfused, processed, frozen, sectioned at 40 microns, and imaged at 40 micron intervals. Focal openings in the blood brain barrier appeared as small, well-circumscribed, blue regions in the brain tissue (results not shown)

Evans Blue dye staining was also assessed with larger 2mm sections and scanning of the tissue. In this experiment, rat brains were treated with Evans Blue dye, were perfused, processed, frozen, sectioned at 2mm intervals, and scanned. Blood brain barrier opening appears to be demonstrated in the section number 4 and 11 (fig. 7 A-B). As evidenced in this tissue, blue does not appear to be evident on the opposite side of the either section 4 or 11. This would likely

indicate that the blood brain barrier opening from anterior to posterior was less than 2mm in length.

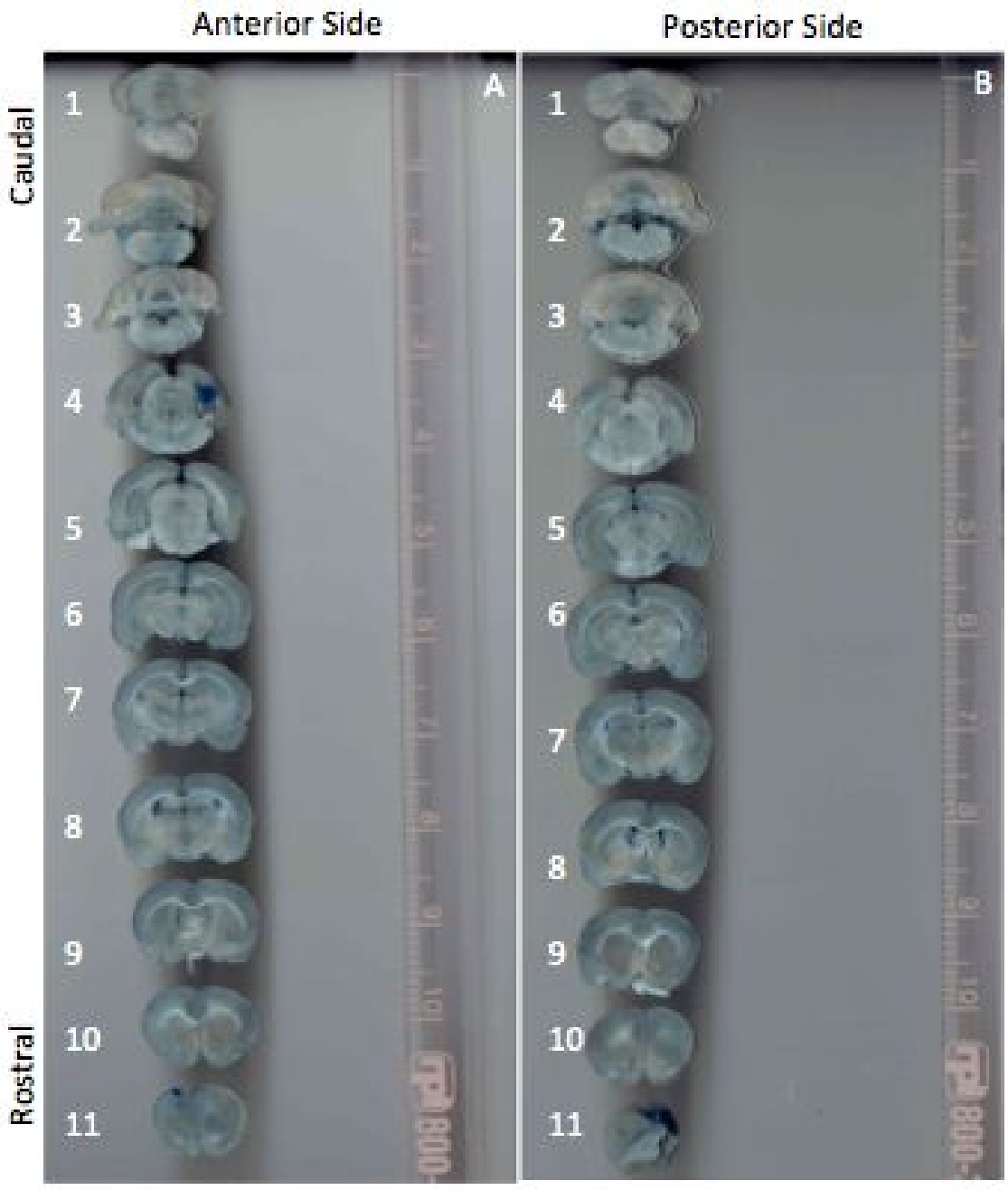


Figure 7. 2mm coronal sections of Sprague Dawley rat after treatment with pulsed focused ultrasound. Scale on right is in cm. From top to bottom, sections are arranged from caudal to rostral. (A) Anterior (rostral) side of section. (B) Posterior (caudal) side of section. Evidence of Evans Blue extravasation appears evident on the anterior side of section 4, right side of section. Section 11 may also demonstrate evidence of Evans Blue extravasation.

# Discussion

Investigation into pulsed focused ultrasound (pFUS) as a therapy for chronic stroke is ongoing. The results presented here are preliminary to understanding what role pFUS may have in treating stroke.

Attempting to visualize differences in cellular antigens could provide clues on how pulsed focused ultrasound therapy could be utilized and optimized. Staining for changes in neuroprogenitor cell markers like Nestin and Doublecortin will show us how endogenous stem cell populations may change with treatment. Costaining with targets like Ki-67 would provide insight as to whether changes in neuroprogenitor cell populations are associated with proliferation. Visualizing shifts in other endogenous cell populations with staining for markers like CD11b/c, GFAP, MBP, NF-68, and Calbindin, could also help elucidate what cellular changes may result from pFUS treatment of brain tissue.

Attempting to visualize differences in the markers SDF-1 and CXCR4 will help us elucidate how endogenous release of SDF-1 may be used for exogenous recuitment of UCBSCs. If recruitment of endogenous, Nestin-positive cells is upregulated via SDF-1:CXCR4, then additional experiments with exogenous stem cell populations would be worth investigating. This would be because the release of SDF-1 as a result of pFUS could improve UCBSCs homing to sites of chronic stroke. If this homing were to take place, then exogenous stem cells may be able to differentiate into neurons, and glial cells, and restore cellular functions otherwise lost due to stroke.

Other mechanisms that need further elucidation includes the extent to which focal blood brain barrier opening occurs. Initial findings on Evans Blue staining appeared to show blood brain barrier opening, but controls and larger sample sizes are needed in order to establish this.

# Literature Cited

Abbott, N.J., and Romero, I.A. (1996). Transporting therapeutics across the blood-brain barrier. Mol. Med. Today *2*, 106–113.

Aggarwal, S., Yurlova, L., & Simons, M. (2011). Central nervous system myelin: structure, synthesis and assembly. *Trends in cell biology*, *21*(10), 585-593.

Bakay LL, Hueter TF, Ballantine HT, and Sosa DD (1956). Ultrasonically produced changes in the blood-brain barrier. AMA Arch. Neurol. Psychiatry *76*, 457–467.

Ballantine, H.T., Bell, E., and Manlapaz, J. (1960). Progress and Problems in the Neurological Applications of Focused Ultrasound. J. Neurosurg. *17*, 858–876.

Blanchette, M., Michaud, K., and Fortin, D. (2012). A new method of quantitatively assessing the opening of the blood–brain barrier in murine animal models. J. Neurosci. Methods *207*, 125–129.

Bonaventura, G., Chamayou, S., Liprino, A., Guglielmino, A., Fichera, M., Caruso, M., & Barcellona, M. L. (2015). Different Tissue-Derived Stem Cells: A Comparison of Neural Differentiation Capability. *PloS one*, *10*(10), e0140790.

Brown, J. P., Couillard-Després, S., Cooper-Kuhn, C. M., Winkler, J., Aigner, L., & Kuhn, H. G. (2003). Transient expression of doublecortin during adult neurogenesis. *Journal of Comparative Neurology*, *467*(1), 1-10.

Burks, S. R., Ziadloo, A., Kim, S. J., Nguyen, B. A., & Frank, J. A. (2013). Noninvasive pulsed focused ultrasound allows spatiotemporal control of targeted homing for multiple stem cell types in murine skeletal muscle and the magnitude of cell homing can be increased through repeated applications. *Stem Cells*, *31*(11), 2551-2560.

Butovsky, O., Landa, G., Kunis, G., Ziv, Y., Avidan, H., Greenberg, N., ... & Schwartz, M. (2006). Induction and blockage of oligodendrogenesis by differently activated microglia in an animal model of multiple sclerosis. *The Journal of clinical investigation*, *116*(4), 905-915.

Buzanska, L., Jurga, M., Stachowiak, E. K., Stachowiak, M. K., & Domanska-Janik, K. (2006). Neural stem-like cell line derived from a nonhematopoietic population of human umbilical cord blood. *Stem cells and development*, *15*(3), 391-406.

Choi, J.J., Pernot, M., Small, S.A., and Konofagou, E.E. (2007). Noninvasive, transcranial and localized opening of the blood-brain barrier using focused ultrasound in mice. Ultrasound Med. Biol. *33*, 95–104.

Dadwal, P., Mahmud, N., Sinai, L., Azimi, A., Fatt, M., Wondisford, F. E., ... & Morshead, C. M. (2015). Activating endogenous neural precursor cells using metformin leads to neural repair and functional recovery in a model of childhood brain injury. *Stem cell reports*, *5*(2), 166-173.

Dalous, J., Larghero, J., & Baud, O. (2012). Transplantation of umbilical cord-derived mesenchymal stem cells as a novel strategy to protect the

central nervous system: technical aspects, preclinical studies, and clinical perspectives. *Pediatric research*, *71*(4-2), 482-490.

Darsalia, V., Allison, S. J., Cusulin, C., Monni, E., Kuzdas, D., Kallur, T., ... & Kokaia, Z. (2011). Cell number and timing of transplantation determine survival of human neural stem cell grafts in stroke-damaged rat brain. *Journal of Cerebral Blood Flow & Metabolism*, *31*(1), 235-242.

Deber, C. M., & Reynolds, S. J. (1991). Central nervous system myelin: structure, function, and pathology. *Clinical biochemistry*, *24*(2), 113-134.

Dokladny, K., Moseley, P. L., & Ma, T. Y. (2006). Physiologically relevant increase in temperature causes an increase in intestinal epithelial tight junction permeability. *American Journal of Physiology-Gastrointestinal and Liver Physiology*, *290*(2), G204-G212.

Felling, R. J., Snyder, M. J., Romanko, M. J., Rothstein, R. P., Ziegler, A. N., Yang, Z., ... & Levison, S. W. (2006). Neural stem/progenitor cells participate in the regenerative response to perinatal hypoxia/ischemia. *The Journal of neuroscience*, *26*(16), 4359-4369.

Mr. Rene Solano Fonseca, Ms. Swetha Mahesula, Ms. Deana Apple, Rekha Raghunathan, Allison Dugan, Astrid Cardona, Jason O'Connor, and Erzsebet Kokovay (February 2016, ahead of print). Neurogenic niche microglia undergo positional remodeling and progressive activation contributing to age - associated reductions in neurogenesis. *Stem Cells and Development.* doi:10.1089/scd.2015.0319.

Gage, F. H., Kempermann, G., Palmer, T. D., Peterson, D. A., & Ray, J. (1998). Multipotent progenitor cells in the adult dentate gyrus. *Journal of neurobiology*, *36*(2), 249-266.

Gobbi, A., Karnatzikos, G., & Sankineani, S. R. (2014). One-step surgery with multipotent stem cells for the treatment of large full-thickness chondral defects of the knee. *The American journal of sports medicine*, *42*(3), 648-657.

Haritonova, A., Liu, D., & Ebbini, E. S. (2015). In Vivo application and localization of transcranial focused ultrasound using dual-mode ultrasound arrays. *Ultrasonics, Ferroelectrics, and Frequency Control, IEEE Transactions on*, *62*(12), 2031-2042

Hynynen, K., McDannold, N., Vykhodtseva, N., and Jolesz, F.A. (2001). Noninvasive MR imaging-guided focal opening of the blood-brain barrier in rabbits. Radiology *220*, 640–646.

Hynynen, K., McDannold, N., Sheikov, N.A., Jolesz, F.A., and Vykhodtseva, N. (2005). Local and reversible blood–brain barrier disruption by noninvasive focused ultrasound at frequencies suitable for trans-skull sonications. NeuroImage *24*, 12–20.

Ikeda, T., Iwai, M., Hayashi, T., Nagano, I., Shogi, M., Ikenoue, T., & Abe, K. (2005). Limited differentiation to neurons and astroglia from neural stem cells in the cortex and striatum after ischemia/hypoxia in the neonatal rat brain. *American journal of obstetrics and gynecology*, *193*(3), 849-856.

Jain, K.K. (2012). Nanobiotechnology-based strategies for crossing the blood-brain barrier. Nanomed. *7*, 1225+.

Jang, H.J., Lee, J.-Y., Lee, D.-H., Kim, W.-H., and Hwang, J.H. (2010). Current and Future Clinical Applications of High-Intensity Focused Ultrasound (HIFU) for Pancreatic Cancer. Gut Liver *4*, S57–S61.

Johannessen, A. L., & Torp, S. H. (2006). The clinical value of Ki-67/MIB-1 labeling index in human astrocytomas. *Pathology & Oncology Research*, *12*(3), 143-147.

Kiyatkin, E. A., & Sharma, H. S. (2009). Permeability of the blood–brain barrier depends on brain temperature. *Neuroscience*, *161*(3), 926-939.

Kroll, R.A., and Neuwelt, E.A. (1998). Outwitting the Blood-Brain Barrier for Therapeutic Purposes: Osmotic Opening and Other Means. Neurosurgery *42(5)*, 1083–1099.

Lapidot, T., & Petit, I. (2002). Current understanding of stem cell mobilization: the roles of chemokines, proteolytic enzymes, adhesion molecules, cytokines, and stromal cells. *Experimental hematology*, *30*(9), 973-981.

Lee, J. Y., Ha, K. Y., Kim, J. W., Seo, J. Y., & Kim, Y. H. (2014). Does extracorporeal shock wave introduce alteration of microenvironment in cell therapy for chronic spinal cord injury?. *Spine*, *39*(26), E1553-E1559.

Leinenga, G., & Götz, J. (2015). Scanning ultrasound removes amyloid-β and restores memory in an Alzheimer's disease mouse model. *Science translational medicine*, *7*(278), 278ra33-278ra33.

Li, L., Wu, S., Liu, Z., Zhuo, Z., Tan, K., Xia, H., ... & Xu, Y. (2015). Ultrasound-targeted microbubble destruction improves the migration and homing of Mesenchymal Stem Cells after myocardial infarction by upregulating SDF-1/CXCR4: A Pilot Study. *Stem cells international*.

Li, Y., Tang, G., Liu, Y., He, X., Huang, J., Lin, X., ... & Wang, Y. (2015). CXCL12 gene therapy ameliorates ischemia-induced white matter injury in mouse brain. *Stem Cells Translational Medicine*, sctm-2015.

Liu, H.-L., Fan, C.-H., Ting, C.-Y., and Yeh, C.-K. (2014). Combining Microbubbles and Ultrasound for Drug Delivery to Brain Tumors: Current Progress and Overview. Theranostics *4*, 432–444.

Lois, C., & Alvarez-Buylla, A. (1993). Proliferating subventricular zone cells in the adult mammalian forebrain can differentiate into neurons and glia. *Proceedings of the National Academy of Sciences*, *90*(5), 2074-2077.

McDannold, N., Vykhodtseva, N., Jolesz, F.A., and Hynynen, K. (2004). MRI investigation of the threshold for thermally induced blood–brain barrier disruption and brain tissue damage in the rabbit brain. Magn. Reson. Med. *51*, 913–923.

McDannold, N., Vykhodtseva, N., Raymond, S., Jolesz, F.A., and Hynynen, K. (2005). MRI-guided targeted blood-brain barrier disruption with focused ultrasound: Histological findings in rabbits. Ultrasound Med. Biol. *31*, 1527–1537.

Moskowitz, M.A., Lo, E.H., and Iadecola, C. (2010). The Science of Stroke: Mechanisms in Search of Treatments. Neuron *67*, 181–198.

Nguyen, B., Burks, S., Kim, S., Bresler, M., Tebebi, P., & Frank, J. (2015). Pulsed focused ultrasound enhances mesenchymal stem cell homing to skeletal muscle in a murine model of muscular dystrophy and homing was suppressed by Ibuprofen. *Journal of Therapeutic Ultrasound*, *3*(Suppl 1), P69.

Ohsawa, K., Imai, Y., Sasaki, Y., & Kohsaka, S. (2004). Microglia/macrophage-specific protein Iba1 binds to fimbrin and enhances its actin-bundling activity. *Journal of neurochemistry*, *88*(4), 844-856.

Olson, S. D., Pollock, K., Kambal, A., Cary, W., Mitchell, G. M., Tempkin, J., ... & Tempkin, T. (2012). Genetically engineered mesenchymal stem cells as a proposed therapeutic for Huntington's disease. *Molecular neurobiology*, *45*(1), 87-98.

Ong, J., Plane, J. M., Parent, J. M., & Silverstein, F. S. (2005). Hypoxic-ischemic injury stimulates subventricular zone proliferation and neurogenesis in the neonatal rat. *Pediatric research*, *58*(3), 600-606.

Patel, K., & Sun, D. (2016). Strategies targeting endogenous neurogenic cell response to improve recovery following traumatic brain injury. *Brain Research*.

Shin, J. H., Park, Y. M., Kim, D. H., Moon, G. J., Bang, O. Y., Ohn, T., & Kim, H. H. (2014). Ischemic brain extract increases SDF-1 expression in astrocytes through the CXCR2/miR-223/miR-27b pathway. *Biochimica et Biophysica Acta (BBA)-Gene Regulatory Mechanisms*, *1839*(9), 826-836.

Sofroniew, M. V., & Vinters, H. V. (2010). Astrocytes: biology and pathology. *Acta neuropathologica*, *119*(1), 7-35.

Tabatabaei, S. N., Girouard, H., Carret, A. S., & Martel, S. (2015). Remote control of the permeability of the blood–brain barrier by magnetic heating of nanoparticles: a proof of concept for brain drug delivery. *Journal of Controlled Release*, *206*, 49-57.Tebebi, P. A., Burks, S. R., Kim, S. J., Williams, R. A., Nguyen, B. A., Venkatesh, P., ... & Frank, J. A. (2015). Cyclooxygenase-2 or Tumor Necrosis Factor-α Inhibitors Attenuate the Mechanotransductive Effects of Pulsed Focused Ultrasound to Suppress Mesenchymal Stromal Cell Homing to Healthy and Dystrophic Muscle. *Stem Cells*, *33*(4), 1173-1186.

Tajiri, N., Quach, D. M., Kaneko, Y., Wu, S., Lee, D., Lam, T., ... & Borlongan, C. V. (2014). Behavioral and histopathological assessment of adult ischemic rat brains after intracerebral transplantation of NSI-566RSC cell lines. *PloS one*, *9*(3), e91408.

Tang, H. L., Wang, Z. G., Li, Q., Ran, H. T., Zheng, Y. Y., Ren, J. L., ... & Zhao, B. (2012). Targeted delivery of bone mesenchymal stem cells by

ultrasound destruction of microbubbles promotes kidney recovery in acute kidney injury. *Ultrasound in medicine & biology*, *38*(4), 661-669.

Teasell, R., Foley, N., Salter, K., Bhogal, S., Jutai, J., and Speechley, M. (2009). Evidence-Based Review of Stroke Rehabilitation: Executive Summary, 12th Edition. Top. Stroke Rehabil. *16*, 463–488.

Verdaguer, E., Brox, S., Petrov, D., Olloquequi, J., Romero, R., de Lemos, M. L., ... & Auladell, C. (2015). Vulnerability of calbindin, calretinin and parvalbumin in a transgenic/knock-in APPswe/PS1dE9 mouse model of Alzheimer disease together with disruption of hippocampal neurogenesis. *Experimental gerontology*, *69*, 176-188.

Vykhodtseva, N.I., Hynynen, K., and Damianou, C. (1995). Histologic effects of high intensity pulsed ultrasound exposure with subharmonic emission in rabbit brain in vivo. Ultrasound Med. Biol. *21*, 969–979.

Wang, G., Zhang, Q., Zhuo, Z., Wu, S., Xu, Y., Zou, L., ... & Gao, Y. (2016). Enhanced Homing of CXCR-4 Modified Bone Marrow–Derived Mesenchymal Stem Cells to Acute Kidney Injury Tissues by Micro-Bubble–Mediated Ultrasound Exposure. *Ultrasound in medicine & biology*, *42*(2), 539-548.

Winn, H. R., & Youmans, J. R. (2011). *Youmans neurological surgery* (6th ed.). Philadelphia, PA: Elsevier/Saunders.

Wrenn, S.P., Dicker, S.M., Small, E.F., Dan, N.R., Mleczko, M., Schmitz, G., and Lewin, P.A. (2012). Bursting bubbles and bilayers. Theranostics *2*, 1140–1159.

Xue, L., Wang, J., Wang, W., Yang, Z., Hu, Z., Hu, M., & Ding, P. (2014). The effect of stromal cell-derived factor 1 in the migration of neural stem cells. *Cell biochemistry and biophysics*, *70*(3), 1609-1616.

Yuan, A., Rao, M. V., & Nixon, R. A. (2012). Neurofilaments at a glance. *Journal of cell science*, *125*(14), 3257-3263.

Zhang, Y., Ye, C., Wang, G., Gao, Y., Tan, K., Zhuo, Z., ... & Li, P. (2013). Kidney-targeted transplantation of mesenchymal stem cells by ultrasound-targeted microbubble destruction promotes kidney repair in diabetic nephropathy rats. *BioMed research international*, *2013*.